A Waveguide Mesh Model of High-Frequency Violin Body Resonances

Patty Huang, Stefania Serafin and Julius O. Smith III
CCRMA, Stanford University, CA, USA

pph@ccrma.stanford.edu, serafin@ccrma.stanford.edu, jos@ccrma.stanford.edu

Abstract

In this paper we propose a new technique to build a complex resonator such as the body of a violin.

1 Introduction

An important element of a violin is its body, which filters vibrations that propagate from the string through the bridge. In real-time synthesis of a violin, there is some difficulty in modeling the body because of a tradeoff between accuracy and computational cost. If all the resonances of the body are accounted for by modeling each one with its own pair of filter poles, the computational cost is too high. On the other hand, one cannot implement too few filter poles and neglect the large number of resonances, because the complex filtering of the body contributes strongly to the characteristic timbre of the violin.

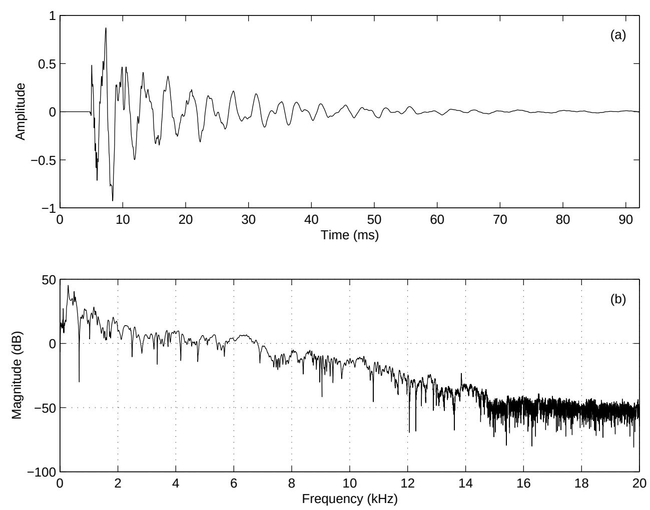

Figure 1: (a) impulse response of a violin body. (b) frequency response of a violin body.

2 Violin Body Resonances

The violin body acts as a resonator for the vibration generated from the strings. The coupling of air cavity modes and top and back plate modes produces the complex filtering which contributes strongly to the characteristic timbre of the violin. At lower frequencies (below 3kHz), the wood modes predominate, and at higher frequencies (above 3kHz) the air modes predominate [HKW95].

The impulse response of a violin body is shown in Fig. 1. The response was obtained by exciting the body vertically with an impulse hammer in an anechoic chamber. The bottom of the figure shows the frequency response. Note the high number of high-frequency resonances.

2.1 Resonance Perception

At low frequencies, the ear is sensitive to the precise tuning of the resonant modes because its frequency resolution is high in this range. At higher frequencies, however, the frequency resolution of the ear is coarser, and a “reasonable” approximation of the spectral envelope shape can be perceptually equivalent, provided the time-domain characteristics (determined by resonance bandwidths and phases) are also sufficiently similar perceptually.

3 Structure of the Model

Our body model is attached to the waveguide bowed string model described in [SSW99]. In the body model, second-order resonant filters model the first 13 resonances (up to about 3200Hz), and a waveguide mesh [VS93] is used to approximate the dense modes of the violin body at higher frequencies. The second-order filters simulate primarily wood modes, and the mesh simulates more air modes than wood modes. As a result, a 3D waveguide mesh provides the most accurate asymptotic mode density. However, it is worthwhile to consider whether the high-frequency modes of a 2D mesh may be sufficient psychoacoustically.

The bridge velocity calculated by the bowed string model is fed to the resonant filters and waveguide mesh in parallel, and their outputs are added, as shown in Fig. 2.

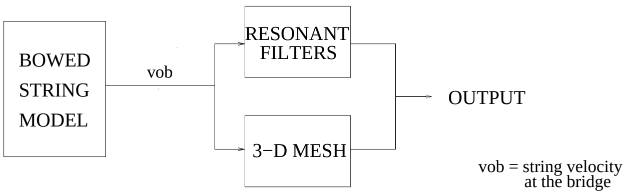

Figure 2: Model Structure.

4 Analysis

The low-frequency resonances are identified and subtracted from the measured violin-body frequency response as described in [KS96]. Using an iterative Matlab program, the loudest resonances are identified and subtracted one by one until the remaining residual impulse response sounds like a noise burst. Figure 3 shows the impulse-response of the resonator-bank and its residual, and Fig. 4 gives the same comparison in the frequency domain. This residual impulse response then becomes the target of a waveguide mesh design.

Figure 3: Impulse Response of (a) Resonator Bank, (b) Residual.

Figure 4: Frequency Response of (a) Resonator Bank, (b) Residual.

5 Mesh Design

The goal of mesh design is to find a mesh having an impulse response which sounds identical to the high-frequency residual obtained after subtracting out the deterministic low-frequency resonators. Due to psychoacoustic properties of hearing, instead of considering individual high-frequency modes, but we may consider bands of high-frequency modes. A reasonable choice is to group high frequency modes into critical bands of hearing according to the Bark [ZF90] or ERB [Moo97] frequency scales. Matlab software for this purpose may be found via [SA99]. Within each band, statistically similar mode distributions can be expected to sound musically equivalent.

Within each band, we wish to match statistics of the mesh response to those of the violin body response. We desire that they be "musically equivalent" based on psychoacoustic principles. The relevant parameters in each band include

- average mode spacing,
- average bandwidth (decay time),
- mode amplitude distribution, and
- mode phase distribution.

For further refinement, the mode bandwidths within each critical band may be characterized statistically as a distribution also (e.g., having a mean and variance); however, our current model does not support this level of detail.

By starting with mesh dimensions comparable to those of a real violin body, we may expect it to spontaneously have a similar mode spacing [Cre84, HKW95]. Additionally, the mode phase should be sufficiently randomized in such a mesh that it is not necessary to explicitly approximate it.

The average absorption can be matched to obtain a the same average decay time in each of several high-frequency bands defining groups of high-frequency modes.

Finally, the mode amplitude distribution can be captured in a spectral envelope, computed, e.g., using linear prediction [Mak75].

6 Simulation results

Figure 8 shows the results of the simulations for a violin E string ($f_0 = 659$ Hz). The top picture displays the waveforms observed at different time intervals of the outgoing velocity at the bridge point, i.e., the waveforms that are entering the mesh and the resonators.

The figures in the center display the outputs of the resonant filters and the mesh respectively, while the figure on the bottom displays the combination of the mesh with the resonant filters.

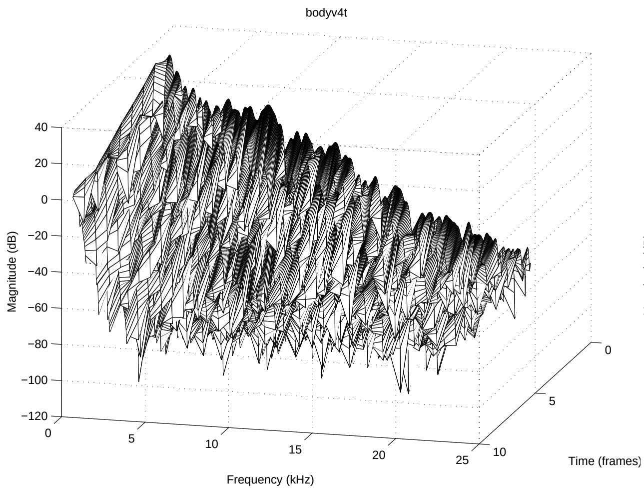

Figure 5: Spectrogram of violin body impulse response.

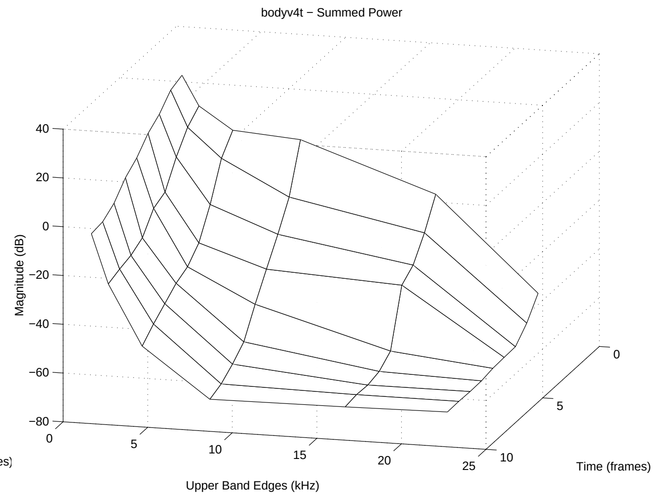

Figure 6: Spectral power decay of violin body impulse response in 6 bands.

The influence of the body model on the spectrum of the bowed string is shown in figure Fig. 9. It is noticeable how the dimensions of the mesh produce a frequency response that has a gap below 2000 Hz and above 8000 Hz.

This hole is related to the fact that the mesh models the high frequency air modes of the cavity.

7 Conclusions

In this paper, we proposed a computationally efficient hybrid model of the violin body. The solution adopted is low-cost without compromising perceptual quality, making our body model suitable for real-time implementation of violin synthesis. This technique can be used to develop synthesis models for other stringed instruments, and any instrument having a complex resonator and a nonlinear excitation which prevents use of commuted synthesis.

References

[Cre84] L. Cremer. The Physics of the Violin. MIT Press, Cambridge, MA, 1984.

[HKW95] A. Hirschberg, J. Kergomard, and G. Weinreich, editors. Mechanics of Musical Instruments. Springer-Verlag, Berlin, 1995.

[KS96] Matti Karjalainen and Julius O. Smith. Body modeling techniques for string instrument synthesis. In Proc. 1996 Int. Computer Music Conf., Hong Kong, pages 232–239. Computer Music Association, Aug. 1996.

[Mak75] J. Makhoul. Linear prediction: A tutorial review. Proc. IEEE, 63:561–580, April 1975.

[Moo97] Brian C. J. Moore. An Introduction to the Psychology of Hearing. Academic Press, New York, 1997.

[SA99] Julius O. Smith and Jonathan S. Abel. Bark and ERB bilinear transforms. IEEE Trans. Speech and Audio Processing, pages 697–708, November 1999. Matlab code for the main figures are available online at http://www-ccrma.stanford.edu/~jos/bbt/.

[Smi97] Julius O. Smith. Nonlinear commuted synthesis of bowed strings. In Proc. 1997 Int. Computer Music Conf., Greece. Computer Music Association, 1997. available online at http://www-ccrma.stanford.edu/~jos/ncbs/.

[SSW99] Stefania Serafin, Julius O. Smith, III, and Jim Woodhouse. An investigation of the impact of torsion waves and friction characteristics on the playability of virtual bowed strings. In Proc. IEEE Workshop on Appl. Signal Processing to Audio and Acoustics, New Paltz, NY, New York, Oct. 1999. IEEE Press.

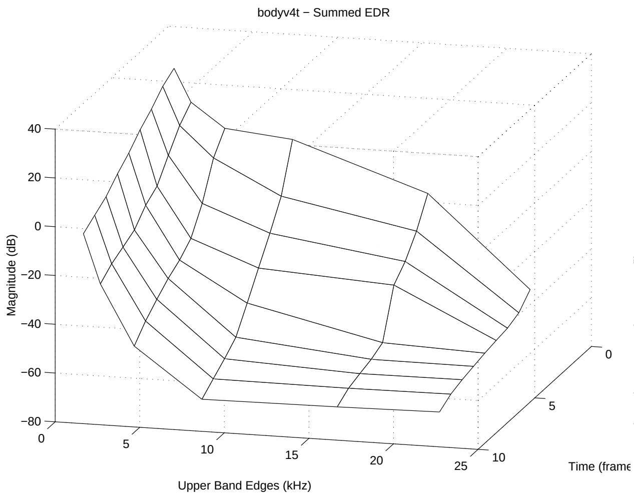

Figure 7: Energy Decay Relief (EDR) for violin body impulse response in 6 bands.

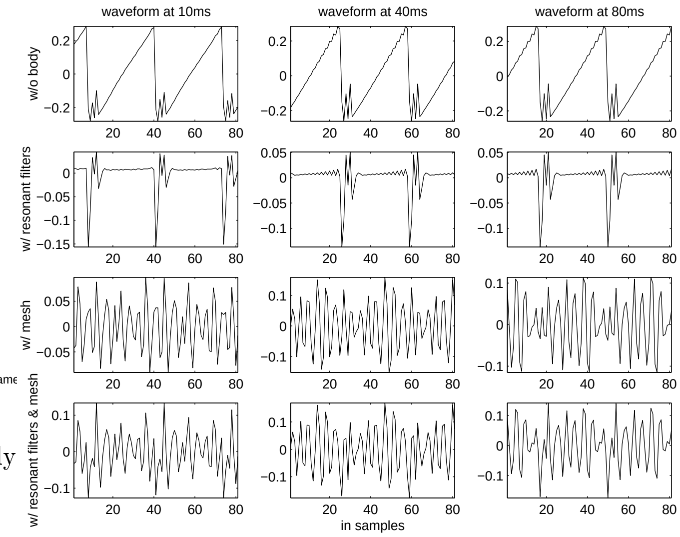

Figure 8: Waveforms of the velocity captured at different locations of the model. From the top: outgoing string velocity at the bridge point, velocity output of the resonant filters, velocity output of the mesh and total final velocity.

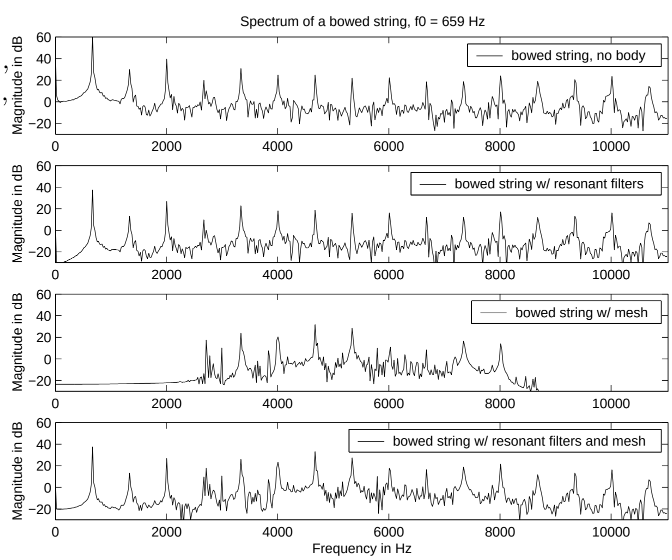

Figure 9: Spectra corresponding to the waveforms of figure Fig. 8.

[SV00] Lauri Savioja and Vesa Välimäki. Reducing the dispersion error in th digital waveguide mesh using interpolation and frequency-warping techniques. IEEE Trans. Speech and Audio Processing, pages 184–194, March 2000.

[VS93] S. A. Van Duyne and Julius O. Smith. Physical modeling with the 2-D digital waveguide mesh. In Proc. 1993 Int. Computer Music Conf., Tokyo, pages 40–47. Computer Music Association, 1993.

[ZF90] E. Zwicker and H. Fastl. Psychoacoustics, Facts and Models. Springer Verlag, Berlin, 1990. see also later 1999 edition.